ELSEVIER

Microelectronic Engineering 61–62 (2002) 529–536

MICROELECTRONIC ENGINEERING

www.elsevier.com/locate/mee

Fabrication and optical measurements of silicon on insulator photonic nanostructures

D. Peyrade[a,*], Y. Chen[a], A. Talneau[a], M. Patrini[b], M. Galli[b], F. Marabelli[b], M. Agio[b], L.C. Andreani[b], E. Silberstein[c], P. Lalanne[c]

[a]*Laboratoire de Photonique et de Nanostructures (LPN), CNRS, Route de Nozay, 91460 Marcoussis, France*
[b]*INFM and Dipartimento di Fisica A. Volta, Università degli Studi di Pavia, Via Bassi 6, I-27100 Pavia, Italy*
[c]*Institut d'Optique, Laboratoire Charles Fabry, BP 147, 91403 Orsay, France*

Abstract

We report on results of the fabrication and optical measurements of silicon on insulator (SOI) nanostructures designed for photonic applications. Patterning has been done by electron beam lithography and reactive ion etching with an SF_6 and CHF_3 gas mixture. Both one dimensional (1D) and two dimensional (2D) photonic lattices were studied by measuring dispersion curves above the light cone. Lateral Fabry-Perot resonators were also fabricated in a waveguide geometry, showing strong dependence of the transmission intensity as a function of the silicon filling factor and the number of air gaps in the Bragg-like mirrors. © 2002 Elsevier Science B.V. All rights reserved.

Keywords: Nanofabrication; Silicon on insulator (SOI); Photonic crystals

1. Introduction

Silicon on insulator (SOI) is now used for the fabrication of high performance microelectronic integrated circuits. Because of the large refraction index difference between silicon and silicon dioxide (insulator), the SOI structures support pure guided modes without coupling to external radiation field [1]. For this reason, SOI is also considered as a potential candidate to develop optical functionalities in the so-called planar photonic integrated circuits (PICs) for advanced telecom applications. On the other hand, a growing interest has been emerging in the study of photonic crystals based on various nanofabrication technologies [2]. For example, by using state-of-the-art electron beam lithography and reactive ion etching techniques, patterning of two dimensional (2D) photonic crystals has succeeded with GaAs, InP and other semiconductor compounds [3–5]. More recently, investigation has also been

*Corresponding author.
E-mail address: david.peyrade@lpn.cnrs.fr (D. Peyrade).

0167-9317/02/$ – see front matter © 2002 Elsevier Science B.V. All rights reserved.
PII: S0167-9317(02)00539-7

focused on SOI type structures [6] because of the possibility of making PICs fully compatible with VLSI chips.

In this work, we study both one dimensional (1D) and two dimensional (2D) photonic lattices fabricated on an SOI substrate. Experimental data of photonic dispersion will be compared to theory based on a plane wave calculation. We will also show transmission spectra of lateral Fabry-Perot resonators of different silicon filling factors and numbers of air-gaps in the Bragg-like mirrors.

2. Fabrication

Silicon on insulator wafers used in this work were manufactured by SOITEC. We have chosen to pattern two SOI layers: L1 consists of a 0.26 μm-thick silicon top layer (waveguide core) and a 1 μm-thick SiO_2 insulator layer supported by a bulk silicon substrate; L2 is formed by a 0.34 μm-thick silicon top layer and a 1 μm-thick SiO_2 layer on a silicon substrate. Patterning has been done by electron beam lithography with a JEOL JBX5D2U vector scan generator at 50-keV energy on a single layer PMMA resist. Several types of photonic structures have been fabricated. For 1D gratings and 2D graphite lattices of pillars, etching has been done with a nickel mask obtained by lift-off, i.e. evaporating a thin nickel layer and dissolving the PMMA. Triangular lattice of holes has been obtained with a tri-layer (PMMA/Ge/AZ) process by using AZ (UV photoresist) as etching mask [7]. Reactive ion etching of silicon top layer is performed in a Nextral NE110 system with an SF_6 and CHF_3 gas mixture, at a pressure of 10 mT and an RF power of 10 W. The RIE parameters have been optimized to obtain steeper sidewalls of silicon. After etching, nickel (polymer) masks are removed by wet chemical etching with NHO_3 acid (acetone) and all obtained structures are observed by scanning electron microscopy (SEM) before optical measurements.

Fig. 1 shows SEM pictures of four types of photonic structures: (a) 1D grating obtained with SOI layer L1 (period $a = 650$ nm and silicon filling factor $f = 0.82$); (b) graphite lattice obtained with L2 ($a = 1.133$ μm and $f = 0.35$); (c) lateral Fabry-Perot resonator in waveguide geometry for 1.55 μm wavelength which consists of a planar microcavity embedded in two Bragg-like mirrors in the centre of a 1 mm length silicon waveguide; and (d) a triangular lattice of holes in a suspended silicon membrane, obtained after wet etching of the SiO_2 layer with an HF solution.

The optical measurements of samples (a) and (b) have been carried out to obtain specular reflectance at various angles and propagation directions. Sample (c) has been used to evaluate the wavelength filtering by measuring transmission spectra along the waveguide, after thinning down the silicon wafer and cleaving the optical facets.

3. Measurements

3.1. Observation of photonic band structure

We used an optical set-up similar to that proposed by Astratov for the determination of photonic bands of GaAs/AlGaAs gratings and triangular lattice of holes [8–10]. A collimated white lamp is used as the incident light, and specular reflectivity spectra are obtained for different incident angles (θ) in respect to the symmetric direction of the photonic lattice. This method is based on the coupling

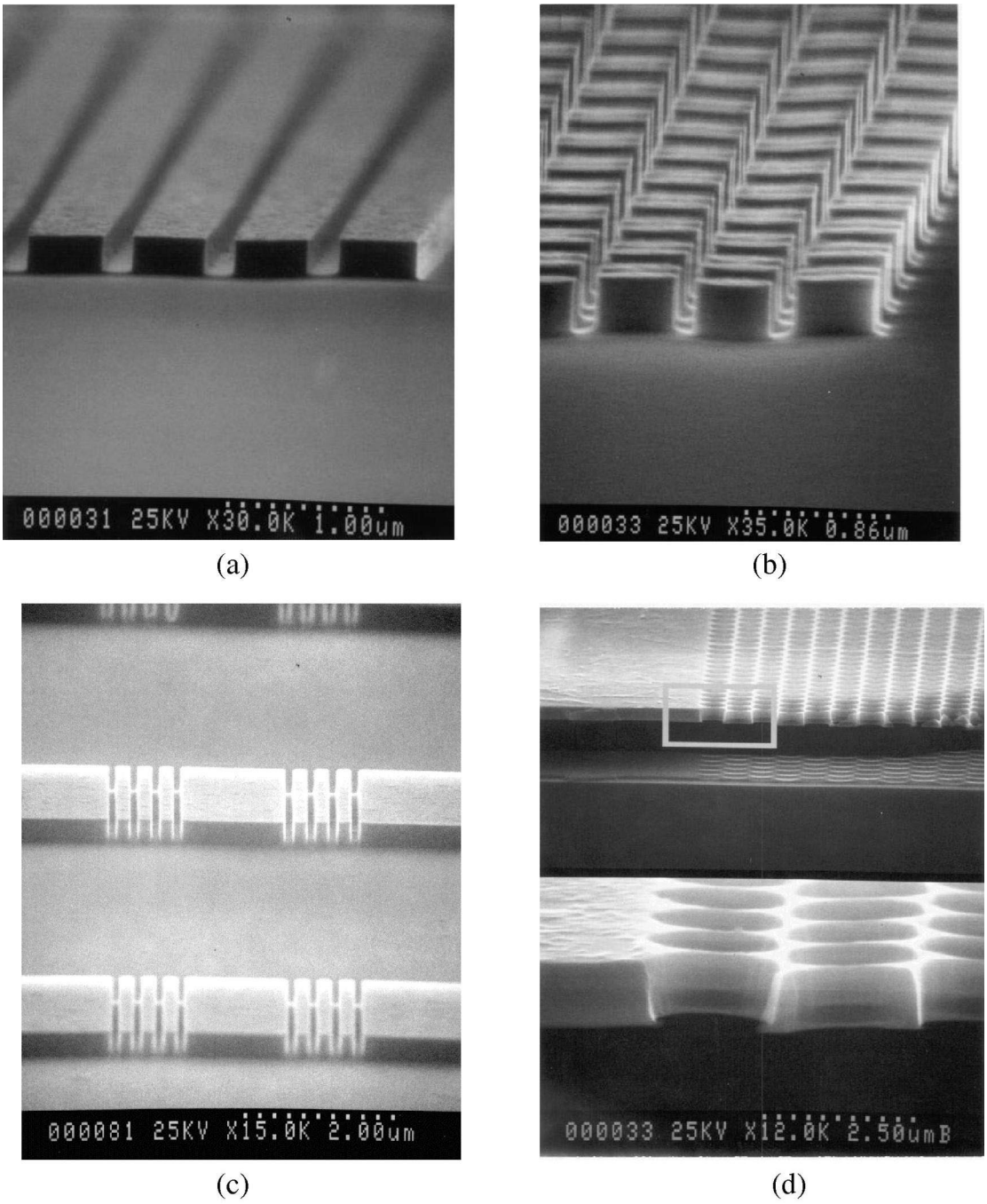

Fig. 1. SEM pictures of (a) grating of 0.65 μm period and 0.82 silicon filling factor made on L1 SOI wafer, (b) 2D graphite lattice of 1.133 μm period and 0.35 filling factor on L2, (c) a wavelength filter in waveguide geometry made on L2, which consists of a cavity of 1.4 μm length and 5 μm width sandwiched between Bragg-like mirrors of four air gaps (270 nm period and 0.66 filling factor), and (d) a triangular lattice of air holes in a silicon suspended membrane on L2.

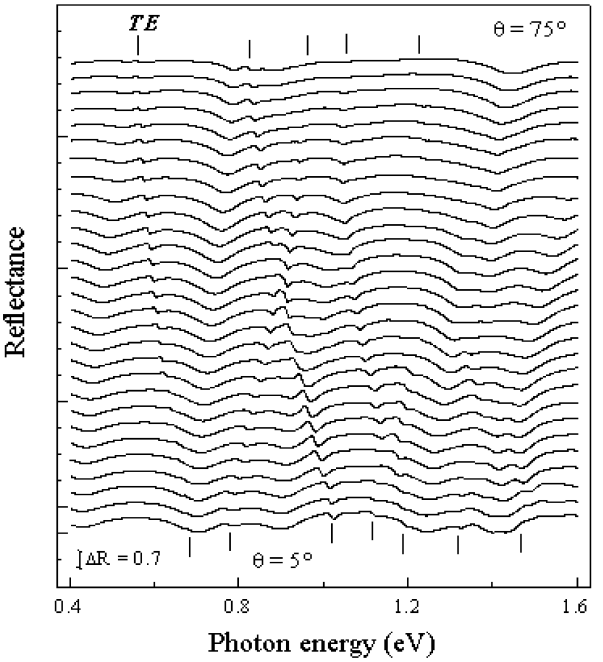

Fig. 2. Specular reflectance spectra of the SOI 1D grating in waveguide configuration (sample a), measured for different incident angles for TE (odd) polarization.

of the external radiation field to a photonic crystal leaky mode, allowing one to build the photonic band structure above the light cone defined by the incident material.

Fig. 2 shows the specular reflectivity of the 1D grating (sample a) as a function of incident photon energy for different angles of incidence (θ) on the grating sample in TE (odd) polarization. Superimposed on the weak interferences of the multilayer system, resonance features can be observed. Those features occur when the frequency ω and the wave-vector component in the plane of the waveguide $k_{//} = \frac{\omega}{c}\sin(\theta)$ matches those of photonic crystal propagating leaky modes. The form (magnitude and width) of these resonances depends critically on the strength of the coupling and give information on the intrinsic radiation losses of the photonic crystal mode [10–12]. Theoretically, all measured features can be reproduced by calculation based on a scattering-matrix method as proposed in Ref. [13]. A detailed comparison between theory and our experimental data can be found elsewhere [12].

By extracting the resonance energies as a function of θ, we can construct the experimental band structure of the photonic lattice by plotting the energies versus the wave vector component $k_{//}$. Fig. 3(a) shows the experimental band structure (solid dots) of the 1D grating defined earlier (for TE polarization and along Γ-X direction). Curves are obtained theoretically based on the plane wave model recently developed by Andreani and Agio [14]. This model is believed to be the most reliable one that allows the calculation of photonic bands above the light cone in a photonic crystal inserted in a waveguide configuration. As can be seen, the experimental and theoretical results are in good agreement. We also note the apparition of the second order photonic bands at 1.04, 1.23 and 1.48 eV

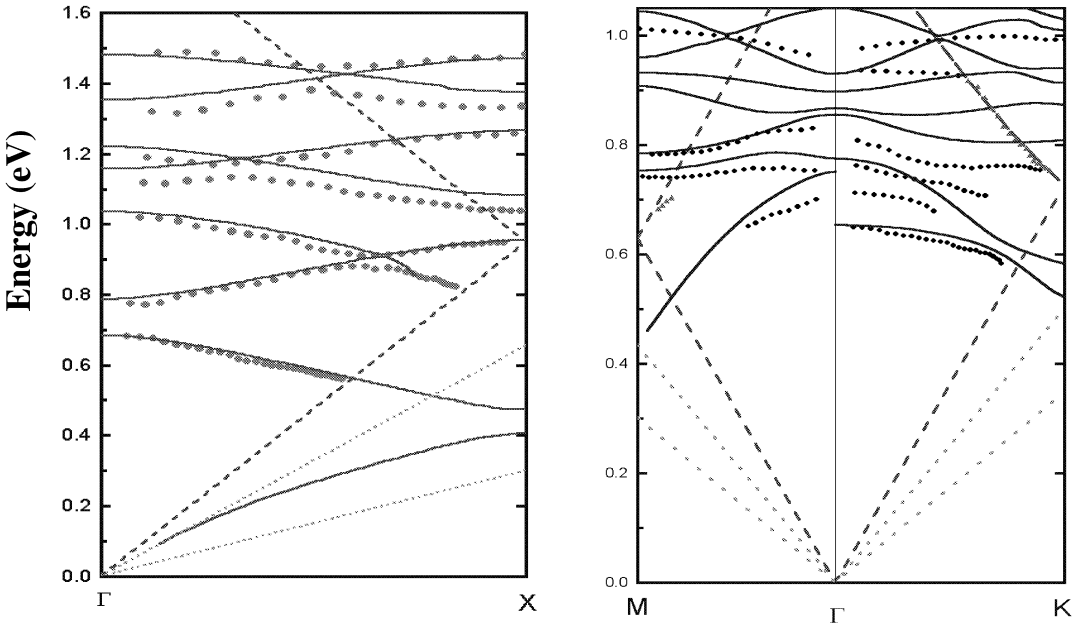

Fig. 3. Photonic band structures of a grating in TE (odd) polarization (a), and a 2D graphite lattice of pillars in TM (even) polarization (b). The experimental data (points) were obtained from reflectance measurements while theoretical curves were calculated using a plane wave model taking into account the dispersion of the silicon refractive index. The dashed lines give the dispersion of light in air while the dotted lines show dispersion of light in Si and SiO_2.

near $\vec{k}_{//} = \vec{0}$. For reasons of symmetry [12], the first and second order photonic bands anticross resulting in very small gaps.

Fig. 3(b) shows the photonic band structure of the graphite lattice (sample b) along Γ-K and Γ-M directions. Here, the agreement between experimental and theoretical calculations is not as good as for the 1D system. One possible explanation is that the small matter filling factor ($f_{Si} = 0.3$) of the PC reduces the effective refractive index of the waveguide core. Then, the resonant features are less pronounced in the reflectivity spectra due to the increase of the diffraction losses outside the waveguide and are more difficult to probe.

3.2. Photonic device in waveguide geometry

A Fabry-Perot resonator is one of the key elements in PICs that allows the isolation of a single channel for a given wavelength. We fabricated a 5 order planar cavity for 1.55-μm wavelength ($L_c = 1.4$ μm), sandwiched between two etched mirrors (sample c). The mirrors were chosen considering the fabrication convenience and the diffraction losses (mirrors' period $a = 270$ nm). In addition, silicon filling factor was increased in the mirrors compared to standard first-order Bragg mirrors to reduce the out-of-plane losses [15].

Fig. 4(a) presents the system response measured with a fiber-to-fiber set-up [16] for SOI

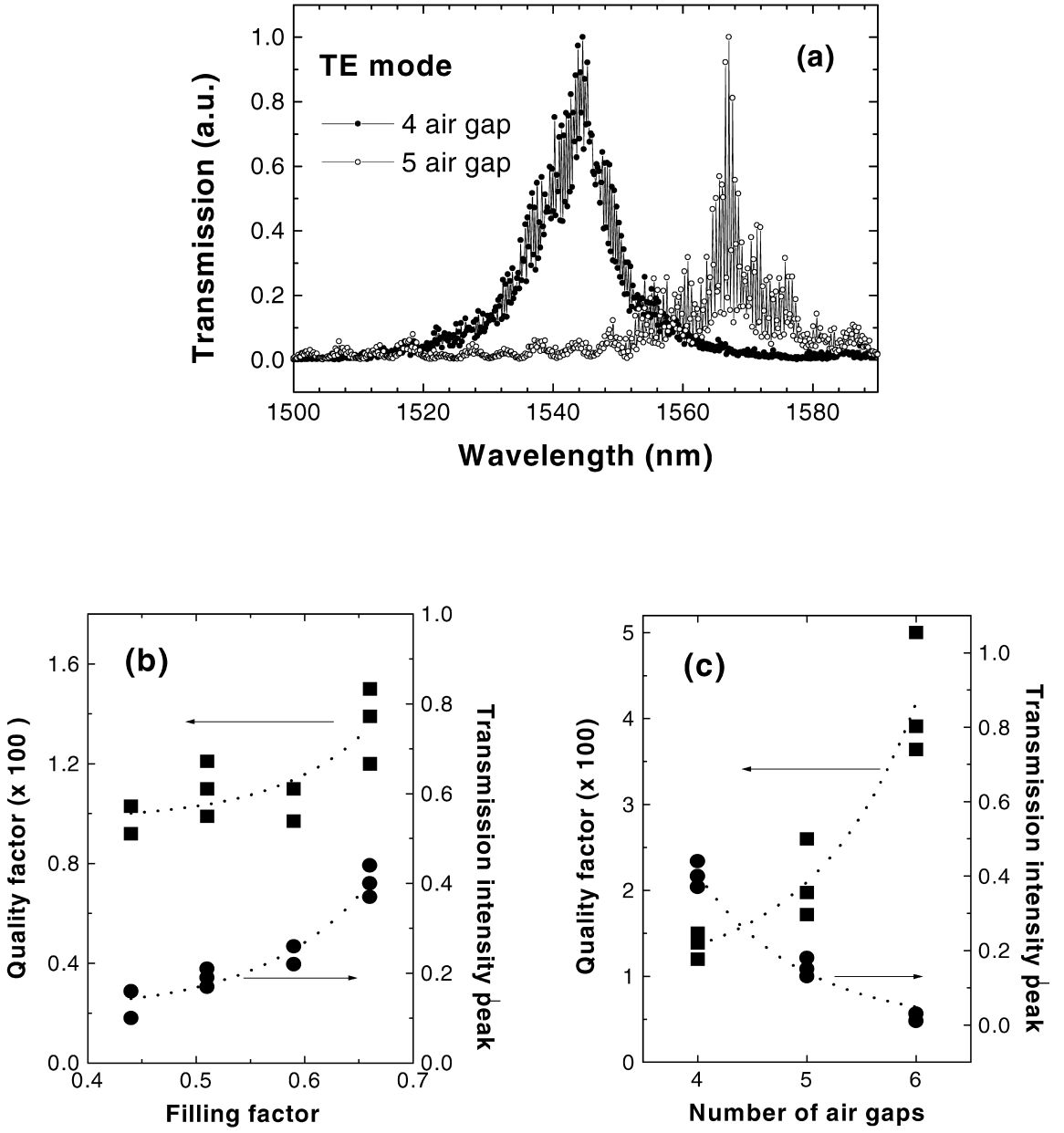

Fig. 4. Results of transmission measurements obtained with the wavelength filter made on L2 (sample c): (a) normalized transmission spectra of the cavity with Bragg-like mirrors of four (solid dots) and five (open dots) air gaps; (b,c) cavity quality factor and transmission peak as a function of the silicon filling factor (b) and the number of air gap (c) of the mirrors.

Fabry-Perot devices with four and five air gaps. Because no numerical treatment has been applied to the measured spectra, high frequency oscillations are visible, which are related to the interference between the two cleaved facets of the waveguide. One can note that the quality factor of the cavity peak defined by $Q = \lambda/\Delta\lambda$ ($\Delta\lambda$ is the width of the resonance) is significantly different in the two

cases: $Q_{4\ \mathrm{air\ gap}}$~140 and $Q_{5\ \mathrm{air\ gap}}$~200. The transmission spectra were then filtered and normalized to a reference waveguide spectrum. Fig. 4(b) gives the transmission peak intensity and quality factor as a function of the silicon filling factor in the mirrors with four air gaps, indicating that higher transmission structures can be achieved by reducing the air gap in the mirrors. The augmentation of the Q-factor is less clear. Absolute transmission of 0.4 and Q-factor of 140 are possible with the largest filling factor, because of better modal matching between the waveguide vertical mode and the photonic Bloch mode. Fig. 4(c) displays the same parameter dependences as a function of the number of air gaps in the mirrors on each side of the cavity. As the numbers of air gap increase, the quality factor of the cavity increases (up to $Q_{6\ \mathrm{air\ gap}}$~450). Nevertheless, normalized transmission collapsed.

A possibility to obtain high transmission has been recently proposed [17] based on the modal adaptation of the photonic crystal Bloch mode and the waveguide mode on one hand, and the cavity mode on the other hand. According to the authors, better Q-factor and higher transmission can be achieved. Fabrication and optical characterization of this structures are in progress.

4. Conclusion

We have shown a simple but reliable material processing for the fabrication of photonic nanostructures based on SOI systems. Several types of planar photonic structures have been obtained and studied by optical spectroscopy. In free-space propagation, we obtained photonic band structures above the light cone on both 1D and 2D lattices inserted in a waveguide and compared them to a theory based on a plane wave model. By measuring the transmission spectra of an SOI Fabry-Perot resonator in the waveguide geometry, we have evaluated the cavity quality factor and the peak transmission intensity as a function of the silicon filling factor and the number of air gaps in the Bragg-like mirrors.

Acknowledgements

One of the authors (D.P.) is also a member of the University of Montpellier, Groupe d'Etude des Semiconducteurs (GES). He gratefully acknowledges Drs D. Coquillat and J. Lascaray (GES) for help and stimulating discussions.

References

[1] S.G. Johnson, S. Fan, P.R. Villeneuve, J.D. Joannopoulos, L.A. Kolodziejski, Phys. Rev. B 60 (24) (1999) 5751.
[2] Photonic crystals, special issue of Adv. Mater., Wiley-VCH, Berlin, 13(6), 2001.
[3] J.R. Wendt, G.A. Vawter, P.L. Gourley, T.M. Brennan, B.E. Hammons, J. Vac. Sci. Technol. B 11 (6) (1993) 2637.
[4] T. Krauss, Y.P. Song, S. Thoms, C.D.W. Wilkinson, R.M. DelaRue, Electron. Lett. 30 (17) (1994) 1444.
[5] T. Baba, IEEE J. Selected Top. Quantum Electron. 3 (3) (1997) 808.
[6] M. Loncar, D. Nedeljkovic, T. Doll, J. Vuckovic, A. Scherer, T. Pearsall, Appl. Phys. Lett. 77 (13) (2000) 1937.
[7] A. Lebib, Y. Chen, F. Carcenac, E. Cambril, L. Manin, L. Couraud, H. Launois, Microelectron. Eng. 53 (2000) 175.
[8] V.N. Astratov, M.S. Skolnick, S. Brand, T.F. Krauss, O.Z. Karimov, R.M. Stevenson, D.M. Whittaker, I.S. Culshaw, R.M. DelaRue, IEEE Proc. Optoelectron. 145 (6) (1998) 398.

[9] V.N. Astratov, D.M. Whittaker, I.S. Culshaw, R.M. Stevenson, M.S. Skolnick, T.F. Krauss, R.M. DelaRue, Phys. Rev. B 60 (24) (1999) 16255.
[10] V.N. Astratov, R.M. Stevenson, I.S. Culshaw, D.M. Whittaker, M.S. Skolnick, T.F. Krauss, R.M. DelaRue, Appl. Phys. Lett. 77 (2) (2000) 178.
[11] V. Pacradouni, W.J. Mandeville, A.R. Cowan, P. Paddon, J.F. Young, S.R. Johnson, Phys. Rev. B 62 (7) (2000) 4204.
[12] M. Patrini, M. Agio, L.C. Andreani, M. Galli, F. Marabelli, D. Peyrade, Y. Chen, IEEE J. Quantum Electron. (in press).
[13] D.M. Whittaker, I.S. Culshaw, Phys. Rev. B 60 (4) (1999) 2610.
[14] L.C. Andreani, M. Agio, IEEE J. Quantum Electron. (in press).
[15] T. Krauss, R.M. DelaRue, Appl. Phys. Lett. 68 (12) (1996) 1613.
[16] A. Talneau, L. Le Gouezigou, N. Bouadma, Opt. Lett. 26 (16) (2001) 1259.
[17] M. Palamaru, P. Lalanne, Appl. Phys. Lett. 78 (11) (2001) 1466.